An exact Riemann solver for multi-material elastic-plastic flows with Mie-Grüneisen equation of state

1. Introduction

In this paper, an exact Riemann solver is built with the consideration of both elastic and plastic waves, for one-dimensional multi-material elastic-plastic materials with the Mie-Grüneisen EOS, isotropic elastic-plastic model [1] and the von Mises' yielding condition.

The elastic-plastic flow is used to describe the deformation process of solid materials under strong dynamics loading, such as explosive or high-speed impact. The simulation of elastic-plastic flows has important application backgrounds, especially in the Implosion Dynamics weapon and Innertial Confine Fusion (ICF). The first try of simulating the elastic-plastic flows was given by Wilkins [1] in 1960s.

Although the control equations of elastic-plastic flow is similar to the equations in computational fluid dynamics (CFD). But there are mainly three difficulties of constructing Riemann solvers in elastic-plastic flows. Firstly, the constitutive models used in elastic-plastic flows are more complicated. Secondly, the EOS for solid materials is also with more characters. Finally, the yielding process of materials may lead to more wave structures.

Recently, a lot of works have been done in constructing approximate Riemann solvers for elastic-plastic flows with the considering of structures in the Riemann problem. For example, Gavrilyuk et al. [2] analyzed the structure of the Riemann solution and constructed a Riemann solver for the linear elastic system of hyperbolic non-conservative models for transverse waves. Cheng et al. [3] analyzed the wave structures of one-dimensional elastic-plastic flows and

developed an effective two-rarefaction approximate Riemann solver with elastic waves (TRRSE). In [4], for one-dimensional elastic-plastic flows, Cheng introduced a HLLCE Riemann solver, which is fast and efficient in resolving elastic waves and plastic waves. Then in [5], Liu et.al remove the unreasonable assumution in HLLCE which may cause big errors in solving multi-material problems and construct a multi-material HLLC elastic-plastic (MHLLCEP) solver.

As we know, in hydrodynamic numerical system, the exact Riemann solver is developed before approximate Riemann solvers [6], and it gives a guide and reference to the developing of approximate solvers. However, in the elastic-plastic flows, for its complexity, there are only a few works have been done in constructing the exact Riemann solver. For example, Garaizar [7] designed an exact Riemann solution of isotropic hyperelastic material theoretically. Miller [8] presented a general iterative method for the solution of the Riemann problem for hyperbolic elastic systems. Gao and Liu [9, 10] firstly considered the yielding condition in, and proposed an exact elastic-perfectly plastic solid Riemann solver with both elastic and plastic states. As many as thirty-six [9] and sixty-four [10] different solution types are considered in their works. However, in their papers, a linear "stiffened-gas" EOS was used in the plastic state and a more simple linear relation of pressure and strain rate is used in the elastic state. This simplification can truly deduce to simple relations across the shock wave and rarefaction wave, but we still need an exact Riemann solver with a uniform and more common used EOS and equations system for different elastic-plastic materials.

In this paper, we want to construct an exact Riemann solver for the elastic-plastic equations system with the isotropic elastic-plastic model and the von Mises' yielding condition. In this system, the Mie-Grüneisen EOS is used for both the elastic state and plastic state of the material, which is an adequate approximation to a wide variety of materials of interest, includes some gaseous or solid explosives and solid metals under high pressure **??**. According to both the theoretical analysation and numerical tests [11], in this system, there may be three to five waves, including one contact wave and elastic wave (shock or

2

rarefaction wave) or plastic wave or both the elastic and plastic waves in each side of the contact wave. We will prove this, the elastic wave always faster than the plastic wave of one side, so varying from the initial condition, there are 6×6 thirty-six possible cases of the structures in the solution. For a given case, we will obtain theoretical relations of all the states as functions of density. At last, through an iteration process of densities at both sides of the contact wave, the exact solution will be obtained. Also, the half Riemann problem and its exact solution are considered in this paper.

This paper is organized as follows. In section 2, we introduce the governing equations to be studied. In section 3, the Riemann problem and the relations for every wave type (contact wave, shock wave and rarefaction wave) is derived. Then, the exact Riemann solver is given in section 4. The half Riemann problem and its solver is introduced in section 5. Some numerical examples are presented to validate the method in section 6. Conclusions are shown in section 7.

2. Governing equations

In this paper, the elastic energy is not included in the total energy. The exclution of the elastic energy is usual for practical engineering problems [12] and is different from that in Ref.[2].

The governing equations system is given as

$$
\begin{cases}
\partial_t \rho + \partial_x(\rho u) = 0, \\
\partial_t(\rho u) + \partial_x(\rho u^2 + p - s_{xx}) = 0, \\
\partial_t(\rho E) + \partial_x\left[(\rho E + p - s_{xx})u\right] = 0, \\
\partial_t s_{xx} + u \partial_x s_{xx} - \dfrac{4}{3}\partial_x u = 0, \\
|s_{xx}| \leq \dfrac{2}{3}Y_0,
\end{cases}
\tag{1}
$$

It contains the following parts.

3

2.1. Conservation terms

For the continuous one-dimensional solid, the conservation terms in differential form can be given as

$$\partial_t \mathbf{U} + \partial_x \boldsymbol{F}(\mathbf{U}) = 0, \ x \in \ \Omega \subset \mathbf{R}, \ t > 0,$$

where

$$\mathbf{U} = \begin{bmatrix} \rho \\ \rho u \\ \rho E \end{bmatrix}, \quad \mathbf{F} = \begin{bmatrix} \rho u \\ \rho u^2 - \sigma \\ (\rho E - \sigma)u \end{bmatrix}, \tag{2}$$

ρ, u, σ and E are the density, velocity in $x-$direction, Cauchy stress and total energy per unit volume, respectively, E has the relation with specific internal energy e as

$$E = e + \frac{1}{2}u^2, \tag{3}$$

$$\sigma = -p + s_{xx}, \tag{4}$$

where p and s_{xx} denote hydrostatic pressure and deviatoric stress in the $x-$direction, respectively.

2.2. The equation of state (EOS)

The relation of the pressure with the density and the specific internal energy is gotten from the equation of state (EOS). In this paper, we consider the Mie-Grüneisen EOS,

$$p(\rho, e) = \rho_0 a_0^2 f(\eta) + \rho_0 \Gamma_0 e, \tag{5}$$

where $f(\eta) = \frac{(\eta-1)(\eta-\Gamma_0(\eta-1)/2)}{(\eta-s(\eta-1))^2}$, $\eta = \frac{\rho}{\rho_0}$, ρ_0, a_0, s and Γ_0 are constant parameters of the Mie-Grüneisen EOS.

2.3. The constitutive relation

Hooke's law is used here to describe the relationship between the deviatoric stress and the strain,

$$\dot{s}_{xx} = 2\mu \left(\dot{\varepsilon}_x - \frac{1}{3}\frac{\dot{V}}{V} \right), \tag{6}$$

where μ is the shear modulus, V is the volume, and the dot means the material time derivative,

$$\dot{()} = \frac{\partial()}{\partial t} + u\frac{\partial()}{\partial t},$$ (7)

and

$$\dot{\varepsilon}_x = \frac{\partial u}{\partial x}, \quad \frac{\dot{V}}{V} = \frac{\partial u}{\partial x}.$$ (8)

By using Eq.(8), Eq.(6) can be rewritten as

$$\frac{\partial s_{xx}}{\partial t} + u\frac{\partial s_{xx}}{\partial t} = \frac{4}{3}\mu\frac{\partial u}{\partial x}.$$ (9)

2.4. The yielding condition

The Von Mises' yielding condition is used here to describe the elastic limit. In one spatial dimension, the von Mises' yielding criterion is given by

$$|s_{xx}| \leq \frac{2}{3}Y_0,$$ (10)

where Y_0 is the yield strength of the material in simple tension.

3. The Riemann problem

The Riemann problem for the 1D time dependent elastic-plastic equations is given as follows:

$$\begin{cases} \partial_t\rho + \partial_x(\rho u) = 0, \\ \partial_t(\rho u) + \partial_x(\rho u^2 + p - s_{xx}) = 0, \\ \partial_t(\rho E) + \partial_x\left[(\rho E + p - s_{xx})u\right] = 0, \\ \partial_t s_{xx} + u\partial_x s_{xx} - \frac{4}{3}\partial_x u = 0, \\ |s_{xx}| \leq \frac{2}{3}Y_0, \\ Q(x, t = 0) = \begin{cases} Q_L, \text{ if } x < 0, \\ Q_R, \text{ if } x \geq 0, \end{cases} \end{cases}$$ (11)

5

where $Q = (\rho, \rho u, \rho E, s_{xx})^T$.

According to the yielding of the material, the equations may have different Jacobian matrix and different sonic velocity. We will discuss them separately.

3.1. Elastic state

3.1.1. Jacobian matrix in elastic regions

For the Mie-Grüneisen EOS, if the material is not yielding,

$$|s_{xx}| < \frac{2}{3} Y_0, \tag{12}$$

the system (11) can be written as

$$\partial_t \mathbf{Q} + \mathbf{J}(\mathbf{Q}) \partial_x \mathbf{Q} = 0, \tag{13}$$

where $Q = (\rho, \rho u, \rho E, s_{xx})$, and the Jacobian matrix is

$$J(Q) = \begin{bmatrix} 0 & 1 & 0 & 0 \\ -u^2 + \frac{\partial p}{\partial \rho} + \Gamma(\frac{u^2}{2} - e) & u(2 - \Gamma) & \Gamma & -1 \\ (\Gamma(\frac{u^2}{2} - e) - e - \frac{u^2}{2} + \frac{\sigma}{\rho} + \frac{\partial p}{\partial \rho})u & -\Gamma u^2 - \frac{\sigma}{\rho} + \frac{u^2}{2} + e & (1 + \Gamma)u & -u \\ \frac{4}{3}\mu\frac{u}{\rho} & -\frac{4}{3}\mu\frac{1}{\rho} & 0 & u \end{bmatrix}, \tag{14}$$

where $\Gamma = \frac{\Gamma_0 \rho_0}{\rho}$.

The eigenvalues of the coefficient matrix $\mathbf{J}(\mathbf{Q})$ are given as

$$\lambda_1 = \lambda_2 = u, \quad \lambda_3 = u - c, \quad \lambda_4 = u + c, \tag{15}$$

where

$$\begin{cases} c_e = \sqrt{a^2 - \frac{\rho_0}{\rho^2}\Gamma_0 s_{xx} + \frac{4}{3}\frac{\mu}{\rho}}, \\ a^2 = \frac{\partial p}{\partial \rho} + \frac{p}{\rho^2}\frac{\partial p}{\partial e} = a_0^2\frac{\partial f}{\partial \eta} + \frac{p}{\rho^2}\rho_0\Gamma_0. \end{cases} \tag{16}$$

6

The corresponding right eigenvectors are

$$
r_1 = \begin{bmatrix} \frac{1}{b_1} \\ \frac{u}{b_1} \\ 0 \\ 1 \end{bmatrix}, \quad
r_2 = \begin{bmatrix} -\frac{\Gamma}{b_1} \\ -\frac{\Gamma u}{b_1} \\ 1 \\ 0 \end{bmatrix}, \quad
r_3 = \frac{1}{\phi^2}\begin{bmatrix} 1 \\ u - c_e \\ h - u c_e \\ \phi^2 \end{bmatrix}, \quad
r_4 = \frac{1}{\phi^2}\begin{bmatrix} 1 \\ u + c_e \\ h + u c_e \\ \phi^2 \end{bmatrix},
\tag{17}
$$

where

$$
b_1 = \frac{\partial p}{\partial \rho} - \Gamma E, \quad h = E + \frac{p - s_{xx}}{\rho},
\tag{18}
$$

and

$$
\phi^2 = a^2 - \frac{\rho_0}{\rho^2}\Gamma_0 s_{xx} - c_e^2 = -\frac{4\mu}{3}\frac{1}{\rho}.
\tag{19}
$$

3.1.2. A relation between ρ and s_{xx}

Thanks to (7), the equations of the density and the deviatoric stress in Eq.(11) can be written as

$$
\frac{\partial u}{\partial x} = -\frac{1}{\rho}\frac{d\rho}{dt},
\tag{20}
$$

and

$$
\frac{ds_{xx}}{dt} = \frac{4}{3}\mu\frac{\partial u}{\partial x}.
\tag{21}
$$

Substituting (20) into (21) yields

$$
\frac{ds_{xx}}{dt} = -\frac{4}{3}\mu\frac{1}{\rho}\frac{d\rho}{dt}.
\tag{22}
$$

Integrate the above equation from the data in front of a wave to the data behind the wave and perform some simple algebraic manipulations, one can get

$$
s_{xx} + \frac{4}{3}\mu\ln(\rho) = \text{constant}
\tag{23}
$$

This relation always hold in the elastic state.

3.1.3. Relations across the contact wave

For a system without molecular diffusion, there is no materials convecting across the contact wave or interface, so the velocities on two sides of the discontinuity are always equal. This can also be verified by the eigenvectors in Eq.(17) and Eq.(71).

Using $\mathbf{W}_L^*$ and $\mathbf{W}_R^*$ to denote the two data states connected the contact wave, where $\mathbf{W} = (\rho, u, p, s_{xx})$.

Thanks to Eq.(17), for the λ_1-wave we have

$$\frac{d\rho}{\frac{1}{b_1}} = \frac{d\rho u}{\frac{u}{b_1}} = \frac{d\rho E}{0} = \frac{ds_{xx}}{1}. \tag{24}$$

From the above equations, we can easily deduce that

$$du = 0, \quad d(s_{xx} - p) = 0, \tag{25}$$

which means

$$u_L^* = u_R^*, \tag{26}$$

and

$$\sigma_{x,L}^* = \sigma_{x,R}^*, \tag{27}$$

where $()_L^*$ and $()_R^*$ denote $()$ in the region of $\mathbf{W}_L^*$ and $\mathbf{W}_R^*$, respectively. Here we do not show the details of the derivation for a simple presentation.

Similarly, for the λ_2-wave one has

$$\frac{d\rho}{\frac{-\Gamma}{b_1}} = \frac{d\rho u}{\frac{-u\Gamma}{b_1}} = \frac{d\rho E}{1} = \frac{ds_{xx}}{0}. \tag{28}$$

From the above equations, we can easily deduce that

$$du = 0, \quad dp = 0, \quad ds_{xx} = 0, \tag{29}$$

which means

$$u_L^* = u_R^*, \tag{30}$$

8

$$p_L^* = p_R^*, \quad s_{xx,L}^* = s_{xx,R}^*. \tag{31}$$

From Eq.(31), we get that

$$\sigma_{x,L}^* = \sigma_{x,R}^*. \tag{32}$$

At last, for the λ_1 and λ_2 waves, one can find that the following two relations always hold:

$$u_L^* = u_R^*, \quad \sigma_{x,L}^* = \sigma_{x,R}^*. \tag{33}$$

For convenience, we define

$$s^* = u_L^* = u_R^*. \tag{34}$$

where s^* denotes the velocity of the contact wave.

3.1.4. Relations across rarefaction waves

Left-going rarefaction wave Across the left wave associated with λ_3-wave, $(\lambda_3 = u - c_e)$, we have

$$\frac{d\rho}{1} = \frac{d(\rho u)}{u - c_e} = \frac{d(\rho E)}{h - uc_e} = \frac{ds_{xx}}{-\frac{4\mu}{3}\frac{1}{\rho}}. \tag{35}$$

which lead to

$$\mathrm{d}u = -\frac{c_e}{\rho}\mathrm{d}\rho, \tag{36}$$

$$\mathrm{d}E = -\frac{\sigma + \rho u c_e}{\rho^2}d\rho. \tag{37}$$

$$\mathrm{d}s_{xx} = -\frac{4}{3}\frac{\mu}{\rho}d\rho, \tag{38}$$

Take the relation of EOS (5) in, we can get the pressure as

$$dp = \left(a_0^2\frac{\partial f}{\partial \eta} + \frac{p}{\rho^2}\rho_0\Gamma_0 - \frac{\rho_0}{\rho^2}\Gamma_0 s_{xx}\right)d\rho, \tag{39}$$

it can be written as a differential equation of $p(\rho)$

$$p'(\rho) - \lambda_1 \frac{p}{\rho^2} = f_2(\rho), \tag{40}$$

where

$$\lambda_1 = \rho_0 \Gamma_0 \quad f_2(\rho) = a_0^2 \frac{\partial f}{\partial \eta} - \lambda_1 \frac{s_{xx}(\rho)}{\rho^2}. \tag{41}$$

The pressure can be solved out as

$$p e^{\frac{\lambda_1}{\rho}} - \int f_2(\rho) e^{\frac{\lambda_1}{\rho}} d\rho = \text{constant}. \tag{42}$$

Then for a given density ρ, we can get the sonic speed c_e and velocity

$$u + \int \frac{c_e}{\rho} d\rho = \text{constant}. \tag{43}$$

Right-going rarefaction wave Across the right wave associated with λ_4-wave, $(\lambda_3 = u + c_e)$, we have

$$\frac{d\rho}{1} = \frac{d(\rho u)}{u + c_e} = \frac{d(\rho E)}{h + u c_e} = \frac{d s_{xx}}{-\frac{4\mu}{3} \frac{1}{\rho}}. \tag{44}$$

which lead to

$$\mathrm{d}u = \frac{c_e}{\rho} \mathrm{d}\rho, \tag{45}$$

$$\mathrm{d}E = -\frac{\sigma + \rho u c_e}{\rho^2} d\rho. \tag{46}$$

$$\mathrm{d}s_{xx} = -\frac{4}{3} \frac{\mu}{\rho} d\rho, \tag{47}$$

We can get similar relations as the left-going wave as

$$p e^{\frac{\lambda_1}{\rho}} - \int f_2(\rho) e^{\frac{\lambda_1}{\rho}} d\rho = \text{constant}. \tag{48}$$

$$u - \int \frac{c_e}{\rho} d\rho = \text{constant}. \tag{49}$$

10

3.1.5. Relations across shock waves

Now we consider a shock wave with a speed of s, suppose the state in front of the shock is known as $(\rho_1, u_1, p_1, s_{xx1})$ and the state after the shock is unknown as $(\rho_2, u_2, p_2, s_{xx2})$.

Then use the conservation relation across the wave, which is also known as the Rankine-Hugoniot relation for a shock

$$\rho_2 u_2 = \rho_1 u_1 + s(\rho_2 - \rho_1), \tag{50}$$

$$\rho_2 u_2^2 - \sigma_2 = \rho_1 u_1^2 - \sigma_1 + s(\rho_2 u_2 - \rho_1 u_1), \tag{51}$$

$$(\rho_2 E_2 - \sigma_2)u_2 = (\rho_1 E_1 - \sigma_1)u_1 + s(\rho_2 E_2 - \rho_1 E_1), \tag{52}$$

above relations also can be written as

$$\rho_2(u_2 - s) = \rho_1(u_1 - s), \tag{53}$$

$$\rho_2 u_2(u_2 - s) = \rho_1 u_1(u_1 - s) + \sigma_2 - \sigma_1, \tag{54}$$

$$\rho_2 E_2(u_2 - s) = \rho_1 E_1(u_1 - s) + \sigma_2 u_2 - \sigma_1 u_1, \tag{55}$$

substituting (53) into (54) yields

$$\rho_1(u_2 - u_1)(u_1 - s) = \sigma_2 - \sigma_1, \tag{56}$$

also according to (53), we have

$$u_1 - s = \frac{(u_1 - u_2)\rho_2}{\rho_2 - \rho_1}, \tag{57}$$

then subtituting it into (56)

$$- t(u_2 - u_1)^2 = \sigma_2 - \sigma_1, \tag{58}$$

where $t = \frac{\rho_1 \rho_2}{\rho_2 - \rho_1}$.

Simimar to (56), (55) can be changed into

$$t(u_1 - u_2)(E_2 - E_1) = \sigma_2 u_2 - \sigma_1 u_1. \tag{59}$$

Because of $E = e + \frac{1}{2}u^2$, we can get

$$e_2 - e_1 = -\frac{\sigma_1 + \sigma_2}{2t}. \tag{60}$$

Using the EOS of Mie-Grüneisen (5), can get

$$e = c_0 p - c_1 f(\rho/\rho_0), \tag{61}$$

where $c_0 = \frac{1}{\rho_0 \Gamma_0}$ and $c_1 = \frac{a_0^2}{\Gamma_0}$. Put above equation into (60), we can solve the pressure p_2 out as a function of ρ_2.

$$p_2 = \frac{2t(c_1 f(\rho_2/\rho_0) + e_1) - (\sigma_1 + s_{xx2})}{2tc_0 - 1}, \tag{62}$$

The derivative stress σ_{xx2} also is a function of ρ_2 only. So we can solve the Cauchy stress out as

$$\sigma_2 = -p_2 + s_{xx2}. \tag{63}$$

Then we can use (58) to solve the velocity after the shock

$$u_2 = \begin{cases} u_1 - \sqrt{\dfrac{\sigma_1 - \sigma_2}{t}} & \text{Left-going,} \\[4mm] u_1 + \sqrt{\dfrac{\sigma_1 - \sigma_2}{t}} & \text{Right-going.} \end{cases} \tag{64}$$

And the shock speed is given as

$$s = \frac{\rho_2 u_2 - \rho_1 u_1}{\rho_2 - \rho_1}. \tag{65}$$

By the above deductions of the shock wave, we can get that, if the density after the shock is known, all the unknowns can be solved out.

12

3.2. Plastic state

When the material is yielding, the deviatoric stress is a constant

$$|s_{xx}| = \frac{2}{3}Y_0. \tag{66}$$

And the Riemann problem turns into

$$
\begin{cases}
\partial_t \rho + \partial_x(\rho u) = 0, \\
\partial_t(\rho u) + \partial_x(\rho u^2 + p - s_{xx}) = 0, \\
\partial_t(\rho E) + \partial_x\left[(\rho E + p - s_{xx})u\right] = 0, \\
|s_{xx}| = \frac{2}{3}Y_0, \\
U(x, t = 0) = \begin{cases} U_L, & \text{if } x < 0, \\ U_R, & \text{if } x \geq 0, \end{cases}
\end{cases} \tag{67}
$$

where $\mathbf{U} = (\rho, \rho u, \rho E)$.

3.2.1. Jacobian matrix in plastic regions[1]

The equations (67) can be written as

$$\partial_t \mathbf{U} + \mathbf{J}_p(\mathbf{U})\partial_x \mathbf{U} = 0, \tag{68}$$

where the Jacobian matrix is

$$
\mathbf{J}_p(\mathbf{U}) = \begin{bmatrix}
0 & 1 & 0 \\
-u^2 + \frac{\partial p}{\partial \rho} + \Gamma(\frac{u^2}{2} - e) & u(2 - \Gamma) & \Gamma \\
(\Gamma(\frac{u^2}{2} - e) - e - \frac{u^2}{2} + \frac{\sigma}{\rho} + \frac{\partial p}{\partial \rho})u + \frac{u^2}{2} & -\Gamma u^2 - \frac{\sigma}{\rho} + e & (1 + \Gamma)u
\end{bmatrix}. \tag{69}
$$

The eigenvalues of The eigenvalues of the coefficient matrix $\mathbf{J}_p(\mathbf{Q})$ are given as

$$\lambda_1 = u, \quad \lambda_2 = u - c, \quad \lambda_3 = u + c,$$

---

[1] Code site link

13

where

$$\begin{cases} c_p = \sqrt{a^2 - \dfrac{\rho_0}{\rho^2}\Gamma_0 s_{xx}}, \\ a^2 = \dfrac{\partial p}{\partial \rho} + \dfrac{p}{\rho^2}\dfrac{\partial p}{\partial e} = a_0^2\dfrac{\partial f}{\partial \eta} + \dfrac{p}{\rho^2}\rho_0\Gamma_0. \end{cases} \tag{70}$$

The corresponding right eigenvectors are

$$r_1 = \begin{bmatrix} -\dfrac{\Gamma}{b_1} \\ -\dfrac{\Gamma u}{b_1} \\ 1 \end{bmatrix}, \quad r_2 = \dfrac{1}{h - uc_p}\begin{bmatrix} 1 \\ u - c_p \\ h - uc_p \end{bmatrix}, \quad r_3 = \dfrac{1}{h + uc_p}\begin{bmatrix} 1 \\ u + c_p \\ h + uc_p \end{bmatrix}. \tag{71}$$

where

$$b_1 = \dfrac{\partial p}{\partial \rho} - \Gamma E, \quad h = E + \dfrac{p - s_{xx}}{\rho}. \tag{72}$$

Take a comparason of Eq.(16) and Eq.(70), we notice that the sonic speed is not continuous between the states of elastic and plastic. As the shear modulus μ is always positive, so the elastic wave is always faster than the plastic wave. This is very important and may cause wrong results if ignoring it.

3.2.2. Relations across the contact wave

According to the eigenvectors in Eq.(71), for the λ_1-wave ($\lambda_1 = u$), we have

$$\dfrac{d\rho}{\dfrac{-\Gamma}{b_1}} = \dfrac{d(\rho u)}{\dfrac{-u\Gamma}{b_1}} = \dfrac{d(\rho E)}{1}. \tag{73}$$

From the above equations, we can easily deduce that

$$du = 0, \quad dp = 0. \tag{74}$$

Samilar to that in section **??**, we can also get the relations

$$s^* = u_L^* = u_R^*, \quad \sigma_L^* = \sigma_R^*. \tag{75}$$

14

3.2.3. Relations across rarefaction waves

Left-going rarefaction wave Across the left wave associated with λ_2-wave, $(\lambda_2 = u - c_p)$, we have

$$\frac{d\rho}{1} = \frac{d(\rho u)}{u - c_p} = \frac{d(\rho E)}{h - u c_p}. \tag{76}$$

Samilar to section 3.1.4, we can get the relations

$$pe^{\frac{\lambda_1}{\rho}} - \int f_2(\rho) e^{\frac{\lambda_1}{\rho}} d\rho = \text{constant}. \tag{77}$$

and

$$u + \int \frac{c_p}{\rho} d\rho = \text{constant}, \tag{78}$$

where

$$\lambda_1 = \rho_0 \Gamma_0 \quad f_2(\rho) = a_0^2 \frac{\partial f}{\partial \eta} - \lambda_1 \frac{s_{xx}(\rho)}{\rho^2}. \tag{79}$$

Right-going rarefaction wave Across the right wave associated with λ_3-wave, $(\lambda_3 = u + c_e)$, we have

$$\frac{d\rho}{1} = \frac{d(\rho u)}{u + c_p} = \frac{d(\rho E)}{h + u c_p}. \tag{80}$$

We can get similar relations as the left-going wave as

$$pe^{\frac{\lambda_1}{\rho}} - \int f_2(\rho) e^{\frac{\lambda_1}{\rho}} d\rho = \text{constant}. \tag{81}$$

$$u - \int \frac{c_p}{\rho} d\rho = \text{constant}. \tag{82}$$

3.2.4. Relations across shock waves

By a same deducing process with Section 3.1.5, we can get the state after a shock as

$$s_{xx2} = s_{xx1}, \tag{83}$$

$$p_2 = \frac{2t(c_1 f(\rho_2/\rho_0) + e_1) - (\sigma_1 + s_{xx2})}{2t c_0 - 1}, \tag{84}$$

15

(a) Elastic rarefaction wave (b) Plastic rarefaction wave (c) Both elastic and plastic rarefaction waves

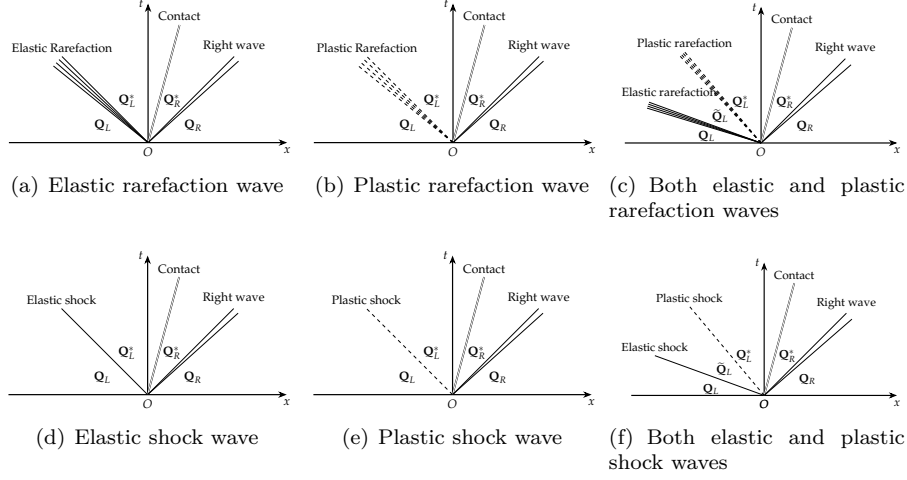(d) Elastic shock wave (e) Plastic shock wave (f) Both elastic and plastic shock waves

Figure 1: The possible cases of Riemann solution structures in the left side.

where $c_0 = \frac{1}{\rho_0 \Gamma_0}$ and $c_1 = \frac{a_0^2}{\Gamma_0}$.

$$\sigma_2 = -p_2 + s_{xx2}. \tag{85}$$

$$u_2 = \begin{cases} u_1 - \sqrt{\dfrac{\sigma_1 - \sigma_2}{t}} & \text{Left-going,} \\[3mm] u_1 + \sqrt{\dfrac{\sigma_1 - \sigma_2}{t}} & \text{Right-going.} \end{cases} \tag{86}$$

And the shock speed is given as

$$s = \frac{\rho_2 u_2 - \rho_1 u_1}{\rho_2 - \rho_1}. \tag{87}$$

4. Exact Riemann solver [2]

Now we consider the constructing details of the exact Riemann solver. For the Riemann problem in Section 4, there are 6×6 possible cases in the Riemann solution with different wave structures. The left six cases are shown in Fig.1.

---

[2] Code site link
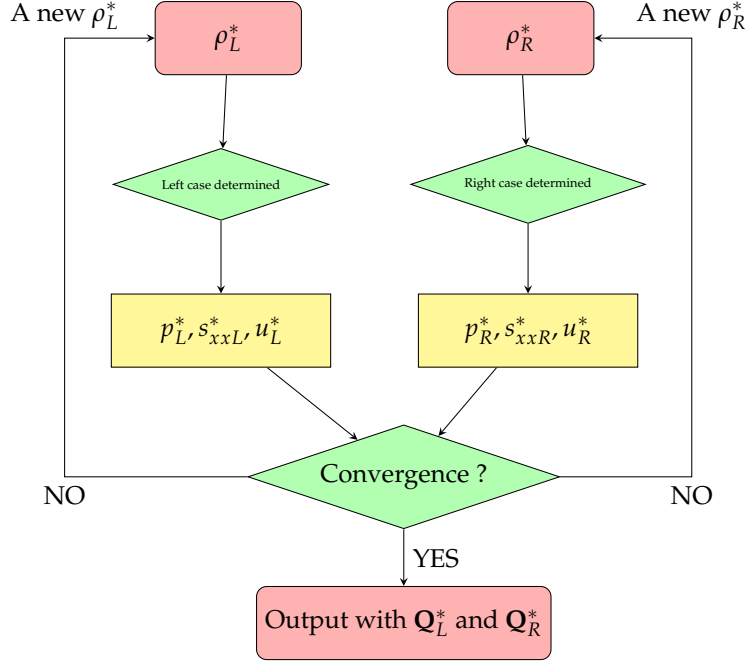
Figure 2: A flow chat of the Newton iteration process.

4.1. The solving process

By the relations in Section 3, all variables can be written as functions of the density, so if densities in regions $\mathbf{R}_L^*$ and $\mathbf{R}_R^*$ are known, the Riemann problem is solved.

For given ρ_L^* and ρ_R^*, by the relation across the contact wave in Section 3.1.3 and Section 3.2.2, we can get

$$
\begin{aligned}
f_u(\rho_L^*, \rho_R^*) &= u_L^* - u_R^* = 0, \\
f_\sigma(\rho_L^*, \rho_R^*) &= \sigma_L^* - \sigma_R^* = 0.
\end{aligned}
\tag{88}
$$

Then using a Newton iteration method, we can solve the densities ρ_L^* and ρ_R^* out. The solving process is shown in Fig.2, and the details are list in the following.

Initial:

The initial densities are given as

$$\rho_{L,(0)}^* = \rho_L \quad \rho_{R(0)}^* = \rho_R.$$ (89)

Iteration begin:

The Newton iteration to evaluate ρ_L^* and ρ_R^* is given as

$$\left[\begin{array}{c} \rho_{L,(k+1)}^* \\ \rho_{R,(k+1)}^* \end{array} \right] = \left[\begin{array}{c} \rho_{L,(k)}^* \\ \rho_{R,(k)}^* \end{array} \right] - \left[\begin{array}{cc} \frac{\partial f_{u(k)}}{\partial \rho_L^*} & \frac{\partial f_{u(k)}}{\partial \rho_R^*} \\ \frac{\partial f_{\sigma(k)}}{\partial \rho_L^*} & \frac{\partial f_{\sigma(k)}}{\partial \rho_R^*} \end{array} \right]^{-1} \left[\begin{array}{c} f_{u(k)} \\ f_{\sigma(k)} \end{array} \right]$$ (90)

The initial of densities are given as

$$\rho_{L(0)}^* = \rho_L \quad \rho_{R(0)}^* = \rho_R.$$ (91)

The convergence is meassured by

$$\mathrm{CHA} = \max \left[\frac{|\rho_{L(k+1)}^* - \rho_{L,(k)}^*|}{\frac{1}{2}|\rho_{L(k+1)}^* + \rho_{L(k)}^*|}, \frac{|\rho_{R(k+1)}^* - \rho_{R,(k)}^*|}{\frac{1}{2}|\rho_{R(k+1)}^* + \rho_{R(k)}^*|}, |f_u|, |f_\sigma| \right].$$ (92)

and the tolerance is taken as $\mathrm{TOL} = 10^{-4}$. It usually takes 3-4 step to get a convergence result.

The derivatives of f_u and f_σ are given by

$$\frac{\partial f_{u,(k+1)}}{\partial \rho_{L(R)}^*} = \frac{f_{u,(k+1)} - f_{u,(k)}}{\rho_{L(R),(k+1)}^* - \rho_{L(R),(k)}^*}, \quad \frac{\partial f_{\sigma,(k+1)}}{\partial \rho_{L(R)}^*} = \frac{f_{\sigma,(k+1)} - f_{\sigma,(k)}}{\rho_{L(R),(k+1)}^* - \rho_{L(R),(k)}^*},$$ (93)

At the first step, we use a simple numerical difference method

$$\frac{\partial f_{u,(1)}}{\partial \rho_{L(R)}^*} = \frac{f_u(\rho_{L(R)}^* + \Delta\rho) - f_u(\rho_{L(R)}^*)}{\Delta\rho_{L(R)}}, \quad \frac{\partial f_{u,(1)}}{\partial \rho_{L(R)}^*} = \frac{f_u(\rho_{L(R)}^* + \Delta\rho) - f_u(\rho_{L(R)}^*)}{\Delta\rho_{L(R)}},$$ (94)

where $\Delta\rho$ is a little quatity, we can choose it as

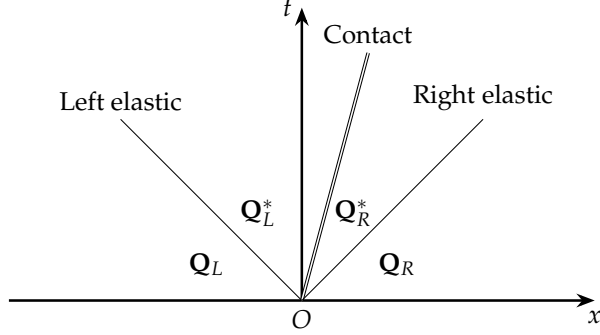$$\Delta\rho_{L(R)} = \frac{\rho_{L(R),(0)}^*}{100}.$$ (95)

18

Figure 3: Pre-evaluation with a three-waves structure.

A flow chat of this process is shown in Fig.2.

4.2. Pre-evaluation of densities

At first, we assume that there are only one elastic shock wave in the left side and another one elastic shock in the right side as shown in Fig.3. According to the conservation relations across the shocks, we have

$$
\begin{cases}
\hat{\rho}_L \hat{u}_L^* = \rho_L u_L + s_L(\hat{\rho}_L^* - \rho_L), \\
\hat{\rho}_L \hat{u}_L^{*2} - \sigma_L^* = \rho_L u_L^2 - \sigma_L + s_L(\hat{\rho}_L^* \hat{u}_L^* - \rho_L u_L),
\end{cases}
\tag{96}
$$

and

$$
\begin{cases}
\hat{\rho}_R \hat{u}_R^* = \rho_R u_R + s_R(\hat{\rho}_R^* - \rho_R), \\
\hat{\rho}_R \hat{u}_R^{*2} - \sigma_R^* = \rho_R u_R^2 - \sigma_R + s_R(\hat{\rho}_R^* \hat{u}_R^* - \rho_R u_R).
\end{cases}
\tag{97}
$$

Using the relation across the interface,

$$
\hat{u}_L^* = \hat{u}_R^* = \hat{s}^*, \quad \hat{\sigma}_L^* = \hat{\sigma}_R^*.
\tag{98}
$$

the speed of contact wave can be evaluated as

$$
\hat{s}^* = \frac{\sigma_L - \sigma_R + \rho_L u_L(s_L - u_L) - \rho_R u_R(s_R - u_R)}{\rho_L(s_L - u_L) - \rho_R(s_R - u_R)},
\tag{99}
$$

19

Table 1: The condition of cases classification.

Conditions	$\|s_{xx}\| < \frac{2}{3}Y_0$ and $\|\hat{s}_{xx}\| < \frac{2}{3}Y_0$	$s_{xx} = \frac{2}{3}Y_0$	other
$\hat{\rho}^* < \rho$	case a	case b	case c
$\hat{\rho}^* > \rho$	case d	case e	case f

the density is solved as

$$\hat{\rho}_L^* = \frac{\rho_L(u_L - s_L)}{\hat{s}^* - s_L}, \quad \hat{\rho}_R^* = \frac{\rho_R(u_R - s_R)}{\hat{s}^* - s_R}. \tag{100}$$

Here we define the speeds of left and right going waves as

$$s_L = \min(u_L - c_L, u_R - c_R, 0), \quad s_R = \max(u_L + c_L, u_R + c_R, 0). \tag{101}$$

4.3. Determining the case of structures

Using a given density ρ_L^*, we can distinguish the shock and rarefaction in the left side. This is done easily by comparing ρ_L^* with ρ_L,

$$\begin{cases} \text{Rarefaction wave:} & \rho_L > \rho_L^*, \\ \text{Shock wave:} & \rho_L < \rho_L^*. \end{cases} \tag{102}$$

To determine the number of waves, we need to know the yielding situation, the devaitoric stress can be evaluated as

$$\hat{s}_{xxL} = -\frac{4}{3}\mu\ln(\frac{\rho_L^*}{\rho_L}) + s_{xxL}, \quad \hat{s}_{xxR} = -\frac{4}{3}\mu\ln(\frac{\rho_R^*}{\rho_R}) + s_{xxR}. \tag{103}$$

Then we can classify every side into six cases, and conditions for the classfication are shown in Table 1, the subscripts $_L$ and $_R$ are omitted for simplication.

4.4. Functions of the pressure, derivative stress and velocity

4.4.1. State in $\tilde{\mathbf{Q}}_{L(R)}$ in cases (c,f)

For cases (c,f), the meterial periods a yielding process from elastic to plastic. There are two waves and one more state $\tilde{\mathbf{Q}}_{L(R)}$ exists. In state $\tilde{\mathbf{Q}}_{L(R)}$, the

20

derivative stress achieves the elastic limit.

$$\tilde{s}_{xxL(R)} = \begin{cases} \dfrac{2}{3}Y_0 & \text{Case (c)}, \\[2ex] -\dfrac{2}{3}Y_0 & \text{Case (f)}, \end{cases} \tag{104}$$

By (23),at state $\tilde{\mathbf{Q}}_{L(R)}$ we can solve the density out as

$$\tilde{\rho}_{L(R)} = \begin{cases} \rho_{L(R)}\exp\left(-\dfrac{Y_0}{2\mu} + \dfrac{3s_{xxL(R)}}{4\mu}\right), & \text{Case (c)}, \\[3ex] \rho_{L(R)}\exp\left(\dfrac{Y_0}{2\mu} + \dfrac{3s_{xxL(R)}}{4\mu}\right), & \text{Case (f)}. \end{cases} \tag{105}$$

Rarefaction wave case (c) For rarefaction wave case, we give the function of s_{xx} at first,

$$s_{xx}(\rho) = -\frac{4}{3}\mu\ln\left(\frac{\rho}{\rho_{L(R)}}\right) + s_{xxL(R)} \quad \rho_{L(R)} \geq \rho \geq \tilde{\rho}_{L(R)} \tag{106}$$

The pressure is given as

$$p(\rho) = p_{L(R)}e^{\frac{\lambda_1}{\rho_{L(R)}} - \frac{\lambda_1}{\rho}} + e^{-\frac{\lambda_1}{\rho}}\int_{\rho_{L(R)}}^{\rho} f_2(x)e^{\frac{\lambda_1}{x}}dx, \quad \rho_{L(R)} \geq \rho \geq \tilde{\rho}_{L(R)}, \tag{107}$$

where

$$\lambda_1 = \rho_0\Gamma_0 \quad f_2(\rho) = a_0^2\frac{\partial f}{\partial \eta} - \lambda_1\frac{s_{xx}(\rho)}{\rho^2}. \tag{108}$$

And sonic speed,

$$c_e(\rho) = \sqrt{a_0^2\frac{\partial f}{\partial \eta} + \frac{p(\rho)}{\rho^2}\rho_0\Gamma_0 - \frac{\rho_0}{\rho^2}\Gamma_0 s_{xx}(\rho) + \frac{4}{3}\frac{\mu}{\rho}} \quad \rho_{L(R)} \geq \rho \geq \tilde{\rho}_{L(R)} \tag{109}$$

Then we can get the function of velocity

$$u(\rho) = \begin{cases} u_L - \displaystyle\int_{\rho_L}^{\rho}\frac{c(x)}{x}dx, & \rho_L \geq \rho \geq \tilde{\rho}_L, \\[3ex] u_R + \displaystyle\int_{\rho_R}^{\rho}\frac{c(x)}{x}dx, & \rho_R \geq \rho \geq \tilde{\rho}_R, \end{cases} \quad \text{case (c)}. \tag{110}$$

21

The states in region $\tilde{\mathbf{Q}}_{L(R)}$ can be solved as

$$\tilde{s}_{xxL(R)} = s_{xx}(\rho_{L(R)}), \quad \tilde{p}_{L(R)} = p(\rho_{L(R)}), \quad \tilde{u}_{L(R)} = u(\rho_{L(R)}). \qquad (111)$$

Shock wave case (f) For shock wave case, the deviatoric stress is given as

$$\tilde{s}_{xxL(R)} = -\frac{4}{3}\mu\ln\left(\frac{\tilde{\rho}_{L(R)}}{\rho_{L(R)}}\right) + s_{xxL(R)} \qquad (112)$$

Then the pressure can be solved as

$$\tilde{p}_{L(R)} = \frac{2t(c_1 f(\tilde{\rho}_{L(R)}/\rho_0) + e_L) - (\sigma_{L(R)} + \tilde{s}_{xxL(R)})}{2tc_0 - 1}, \qquad (113)$$

where $c_0 = \frac{1}{\rho_0\Gamma_0}$, $c_1 = \frac{a_0^2}{\Gamma_0}$ and $t = \frac{\rho_{L(R)}\tilde{\rho}_{L(R)}}{\tilde{\rho}_{L(R)} - \rho_{L(R)}}$.

At last the velocity is

$$\begin{cases} \tilde{u}_L = u_L - \sqrt{\frac{\sigma_L - \tilde{\sigma}_L}{t}}, \\ \tilde{u}_R = u_R + \sqrt{\frac{\sigma_R - \tilde{\sigma}_R}{t}}, \end{cases} \qquad (114)$$

where

$$\tilde{\sigma}_{L(R)} = -\tilde{p}_{L(R)} + \tilde{s}_{L(R)}. \qquad (115)$$

4.4.2. State in $\mathbf{Q}_{L(R)}^*$

For cases (a,b,d,e) in Fig.1, the material is totally yielding or totally not yielding, there is no midlle state $\tilde{\mathbf{Q}}_{L(R)}$. For expression conveience, we let

$$(\tilde{\rho}_{L(R)}, \tilde{u}_{L(R)}, \tilde{p}_{L(R)}, \tilde{s}_{xx}) = (\rho_{L(R)}, u_{L(R)}, p_{L(R)}, s_{xxL(R)}), \qquad (116)$$

in cases (a,b,d,e). Then we can solve the states in region $\mathbf{Q}_{L(R)}^*$ from region $\tilde{\mathbf{Q}}_{L(R)}$ with a given $\rho_{L(R)}^*$.

Rarefaction wave cases (a,b,c) For rarefaction wave, we not only need to solve the state after the wave in region $\mathbf{Q}_{L(R)}^*$, but also need to know the states inside the expansion region.

22

First we give the function of s_{xx},

$$
s_{xx}(\rho) = \begin{cases} -\dfrac{4}{3}\mu \ln\left(\dfrac{\rho}{\tilde{\rho}_{L(R)}}\right) + s_{xxL(R)}, & \tilde{\rho}_{L(R)} \geq \rho \geq \rho^*_{L(R)}, \quad \text{case (a)}, \\[3mm] \dfrac{2}{3}Y_0, & \tilde{\rho}_{L(R)} \geq \rho \geq \rho^*_{L(R)}, \quad \text{case (b,c)}. \end{cases}
$$
(117)

Then we give the pressure,

$$
p(\rho) = \tilde{p}_{L(R)}e^{\frac{\lambda_1}{\rho_{L(R)}} - \frac{\lambda_1}{\rho}} + e^{-\frac{\lambda_1}{\rho}}\int_{\tilde{\rho}_{L(R)}}^{\rho} f_2(x)e^{\frac{\lambda_1}{x}}\,dx, \quad \tilde{\rho}_{L(R)} \geq \rho \geq \rho^*_{L(R)}
$$
(118)

where

$$
\lambda_1 = \rho_0\Gamma_0 \quad f_2(\rho) = a_0^2\frac{\partial f}{\partial \eta} - \lambda_1\frac{s_{xx}(\rho)}{\rho^2}.
$$
(119)

And sonic speed,

$$
c(\rho) = \begin{cases} \sqrt{a_0^2\dfrac{\partial f}{\partial \eta} + \dfrac{p(\rho)}{\rho^2}\rho_0\Gamma_0 - \dfrac{\rho_0}{\rho^2}\Gamma_0 s_{xx}(\rho) + \dfrac{4}{3}\dfrac{\mu}{\rho}} & \text{case (a)}, \\[3mm] \sqrt{a_0^2\dfrac{\partial f}{\partial \eta} + \dfrac{p(\rho)}{\rho^2}\rho_0\Gamma_0 - \dfrac{\rho_0}{\rho^2}\Gamma_0 s_{xx}(\rho)} & \text{case (b,c)}. \end{cases}
$$
(120)

Then we can get the function of velocity

$$
u(\rho) = \begin{cases} \tilde{u}_L - \displaystyle\int_{\rho_L}^{\rho}\dfrac{c(x)}{x}\,dx, & \tilde{\rho}_L \geq \rho \geq \rho^*_L, \\[3mm] \tilde{u}_R + \displaystyle\int_{\rho_R}^{\rho}\dfrac{c(x)}{x}\,dx, & \tilde{\rho}_R \geq \rho \geq \rho^*_R, \end{cases}
$$
(121)

By now, we can get the state in star regions as

$$
p^*_{L(R)} = p(\rho^*_{L(R)}), \quad s^*_{xxL(R)} = s_{xx}(\rho^*_{L(R)}), \quad u^*_{L(R)} = u(\rho^*_{L(R)}).
$$
(122)

Shock wave cases (d,e,f) For shock waves, the deviatoric stress is given as

$$
s^*_{xxL(R)} = \begin{cases} -\dfrac{4}{3}\mu \ln\left(\dfrac{\rho^*_{L(R)}}{\tilde{\rho}_{L(R)}}\right) + \tilde{s}_{xxL(R)}, & \text{case (d)}, \\[3mm] -\dfrac{2}{3}Y_0, & \text{cases (e, f)}. \end{cases}
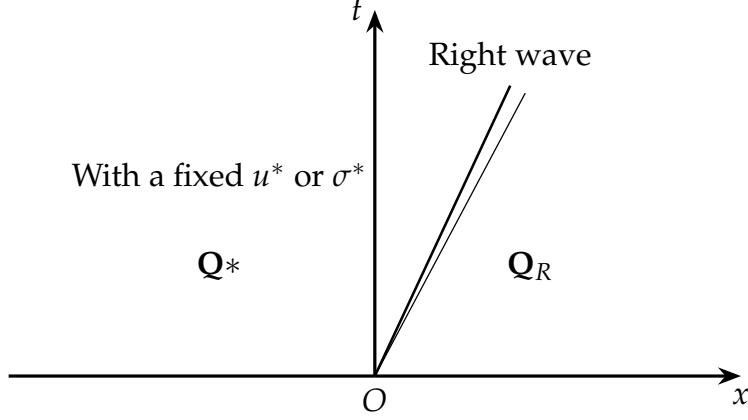$$
(123)

Figure 4: Half Riemann problem with a given left velocity or Cauchy stress..

And the pressure is given as

$$p^*_{L(R)} = \frac{2t(c_1 f(\rho^*_{L(R)}/\rho_0) + \tilde{e}_{L(R)}) - (\tilde{\sigma}_{L(R)} + s^*_{xxL(R)})}{2tc_0 - 1},$$ (124)

where $c_0 = \frac{1}{\rho_0 \Gamma_0}$ and $c_1 = \frac{a_0^2}{\Gamma_0}$ and $t = \frac{\tilde{\rho}_{L(R)} \rho^*_{L(R)}}{\rho^*_{L(R)} - \tilde{\rho}_{L(R)}}$. And the velocity is given as

$$u^*_{L(R)} = \begin{cases} \tilde{u}_L - \sqrt{\frac{\tilde{\sigma}_L - \sigma^*_{L(R)}}{t}}, \\ \tilde{u}_R + \sqrt{\frac{\tilde{\sigma}_R - \sigma^*_{L(R)}}{t}}. \end{cases}$$ (125)

5. Half Riemann problem and its solver

Some times we need to analyse a half Riemann problem with a given velocity or Cauchy stress in one side. Shown in Fig.4 , in these cases, we only need to solve the states in another side. There are six possible cases just like them in Section 4.

The process of solving a half Riemann problem is also in five steps just like the full Riemann problem:

1. First we evaluate the density in the star region $\mathbf{Q}^*$ with a elastic shock assumption.

24
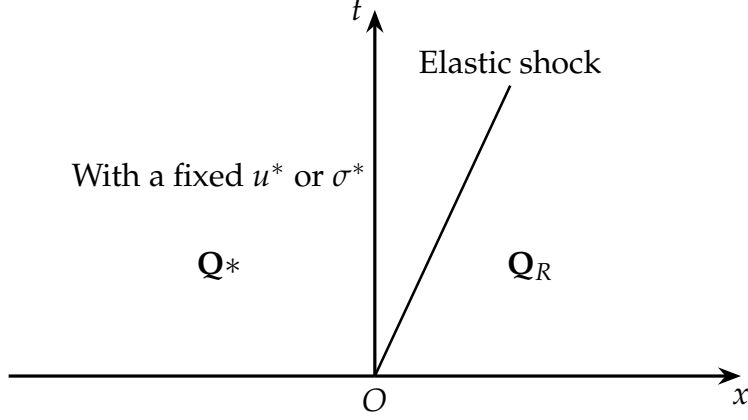
Figure 5: Pre-evaluation of the half Riemann problem with a elastic shock assumeption.

2. By the evaluated density ρ^*, we can determine the structures case.

3. Solving the functions of $\sigma(\rho)$ or $u(\rho)$ according to the wave case.

4. Then using the function of $f_\sigma(\rho^*) = \sigma(\rho^*) - \sigma^*$ (or $f_u(\rho^*) = u(\rho^*) - u^*$) to take a convergent decision, if not, using the Newton iteration process to get a new ρ^* and then take the steps 2-5 again.

5.1. Evaluate of the density $\hat\rho$ in region $\mathbf{Q}^*$

As shown in Fig.5, we assume there is only one elastic shock wave between region $\mathbf{Q}$ and region $\mathbf{Q}^*$.

Then use the shock relation in Section 3.1.5, we can get the functions of Cauchy stress as

$$\sigma(\rho) = -p(\rho) + s_{xx}(\rho), \tag{126}$$

where

$$p(\rho) = \frac{2t(c_1 f(\rho/\rho_0) + e_R) - (\sigma_R + s_{xx}(\rho))}{2tc_0 - 1}, \tag{127}$$

and $c_0 = \frac{1}{\rho_0 \Gamma_0}$ and $c_1 = \frac{a_0^2}{\Gamma_0}$, and $t = \frac{\rho \rho_R}{\rho - \rho_R}$. And the derivative stress is

$$s_{xx}(\rho) = -\frac{4}{3}\mu \ln\left(\frac{\rho}{\rho_R}\right) + s_{xxR}, \tag{128}$$

25

and the velocity is given as

$$u(\rho) = u_R + \sqrt{\frac{\sigma_R - \sigma(\rho)}{t}}. \tag{129}$$

If the Cauchy stress in region $\mathbf{Q}^*$ is given, let

$$f(\rho) = \sigma(\rho) - \sigma_R, \tag{130}$$

if the velocity is given, let

$$f(\rho) = u(\rho) - u_R. \tag{131}$$

The Newton iteration is given as

$$\hat{\rho}_{(k+1)} = \hat{\rho}_{(k)} - f / \frac{\partial f_{(k)}}{\partial \rho}, \tag{132}$$

and the initial is given as

$$\hat{\rho}_{(0)} = \rho_R. \tag{133}$$

The congergence is meassured by

$$\text{CHA} = \max \left[\frac{|\hat{\rho}_{(k+1)} - \hat{\rho}_{(k)}|}{\frac{1}{2}|\hat{\rho}_{(k+1)} + \hat{\rho}_{(k)|}}, |f_{(k+1)}| \right]. \tag{134}$$

5.2. Resolve the state in region $\mathbf{Q}^*$

With a given density ρ^* in region $\mathbf{Q}^*$, a same case determining process is taken as in Section 4.3 to determining the structures case in Table 1. By an exact same iteration process in above

$$\rho^*_{(k+1)} = \rho^*_{(k)} - f / \frac{\partial f_{(k)}}{\partial \rho}, \tag{135}$$

with the initial condition of

$$\rho^*_{(0)} = \hat{\rho}, \tag{136}$$

we can solve the ρ^* out.

In the iteration process the Cauchy stress $\sigma^*(\rho)$ or the velocity $\sigma^*(\rho)$ is given by the relations in Section 4.4 for different cases.

6. Numerical tests

In this section, by choosing suitable initial conditions, we will solve the Riemann problem with several different structure cases in the solution. For simple expression, in figures, we use same representations as those in [10]. "|" means the contact wave, and capital letters "S" and "R" means the shock and rarefaction wave. Superscript letters "E" and "P" indicate the elastic or plastic state of a wave. Numerical results by the method in [5] is used to verified the correctness of the exact solution. In the following tests, the materials are taken as aluminium and copper. The parameters for the EOS and constitutive model for aluminum and copper are $(\rho_0, a_0, \Gamma_0, s, \mu)_{\text{Al}} = (8930\text{kg/m}^3, 3940\text{m/s}, 2, 1.49, 2.76, 2.76 \times 10^{10}\text{Pa})$ and $(\rho_0, a_0, \Gamma_0, s, \mu)_{\text{copper}} = (2785\text{kg/m}^3, 5328\text{m/s}, 2, 1.338, 4.5\times10^{10}\text{Pa})$, respectively. The computational domain is set to be $[0, 1m]$ with 800 cell points and the intial interface is located at $0.5m$, the terminal time is $t = 5 \times 10^{-5}s$.

6.1. Test 1

In this case, the material is yielding at both sides, so the solution structure has three wave with two plastic wave and one contact. The initial condition is

$$\begin{cases} \text{L: Al,} \quad \rho = 2785\text{kg/m}^3, \quad u = 20\text{m/s}, \quad p = 1.0\text{Pa}, \quad s_{xx} = -2.0 \times 10^8\text{Pa,} \\ \text{R: Al,} \quad \rho = 2785\text{kg/m}^3, \quad u = 0\text{m/s}, \quad p = 1.0\text{Pa}, \quad s_{xx} = -2.0 \times 10^8\text{Pa,} \end{cases} \tag{137}$$

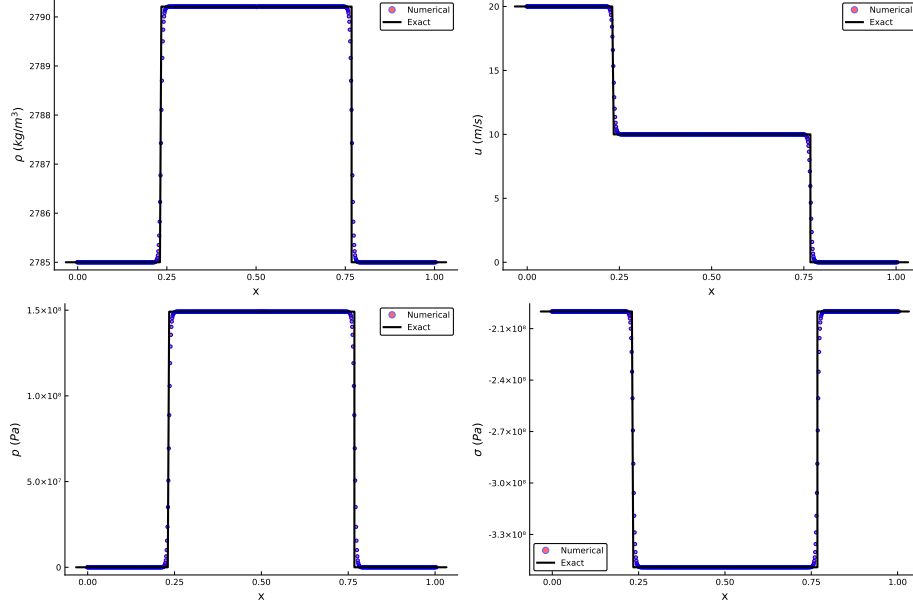It can be seen that the exact solution matches the numerical results very well in Fig.6.

27

Figure 6: Comparison resutls for Test 1 with the structrures of $S^P|S^P$.

6.2. Test 2

Next, we consider a case with yielding process at both sides, so the result has five waves. The initial condition

$$
\begin{cases}
\text{L: Al}, & \rho = 2785\text{kg/m}^3, & u = 800\text{m/s}, & p = 1.0\text{Pa}, & s_{xx} = 0.0\text{Pa}, \\
\text{R: Al}, & \rho = 2785\text{kg/m}^3, & u = 0\text{m/s}, & p = 1.0\text{Pa}, & s_{xx} = 0.0\text{Pa},
\end{cases}
\tag{138}
$$

Shown in Fig.7, the exact solution matches the numerical results well generally, besides the under-cooling effect performed in the numerical results, but it is not considered in the designing of the exact Riemann solver.

6.3. Test 3

In this example, we test the elastic rarefaction waves case. In the structrues there is one elastic rarefaction wave on each side of the contace wave. The initial

28
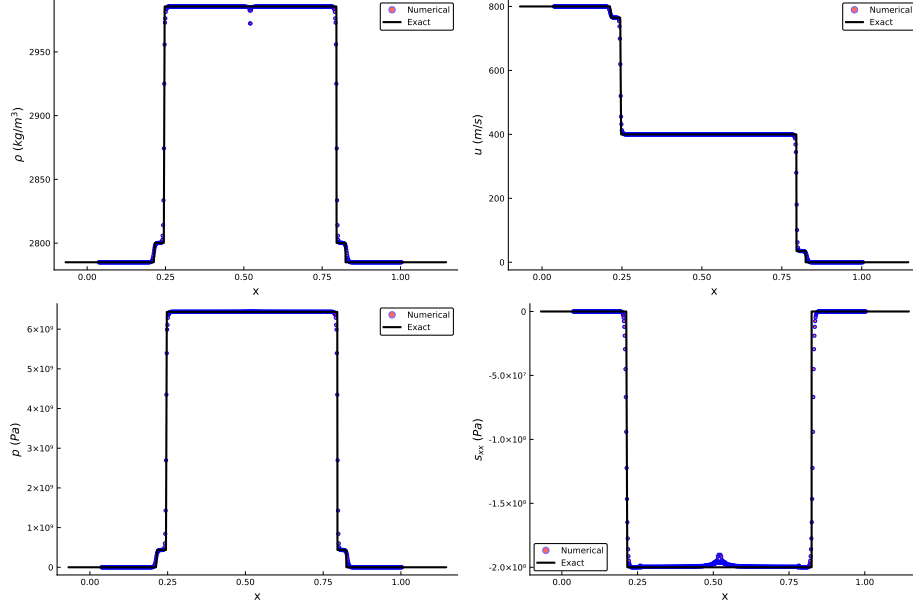
Figure 7: Comparison resutls for Test 1 with the structrures of $S^E S^P | S^P S^E$.

condition is given as

$$
\begin{cases}
\text{L: Al,} & \rho = 2785\text{kg/m}^3, & u = -2.0\text{m/s}, & p = 1.0^7\text{Pa}, & s_{xx} = 0.0\text{Pa}, \\
\text{R: Al,} & \rho = 2785\text{kg/m}^3, & u = 2.0\text{m/s}, & p = 1.0 \times 10^7\text{Pa}, & s_{xx} = 0.0\text{Pa},
\end{cases}
\tag{139}
$$

We can see that the results of the exact solution match the numerical results very well.

6.4. Test 4

Then we test another example with both elastic and plastic rarefaction waves on both sides. The initial condition is

$$
\begin{cases}
\text{L: Al,} & \rho = 2785\text{kg/m}^3, & u = -40\text{m/s}, & p = 1.0 \times 10^7\text{Pa}, & s_{xx} = 0.0\text{Pa}, \\
\text{R: Al,} & \rho = 2785\text{kg/m}^3, & u = 40\text{m/s}, & p = 1.0 \times 10^7\text{Pa}, & s_{xx} = 0.0\text{Pa}.
\end{cases}
\tag{140}
$$

Results are shown in Fig.9, the results of the exact solver matches the numerical results very well.
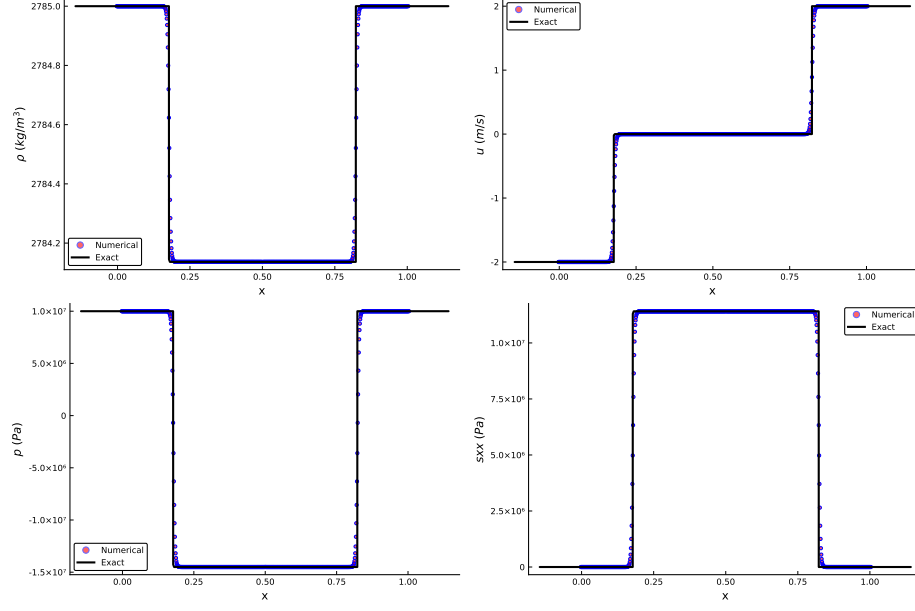
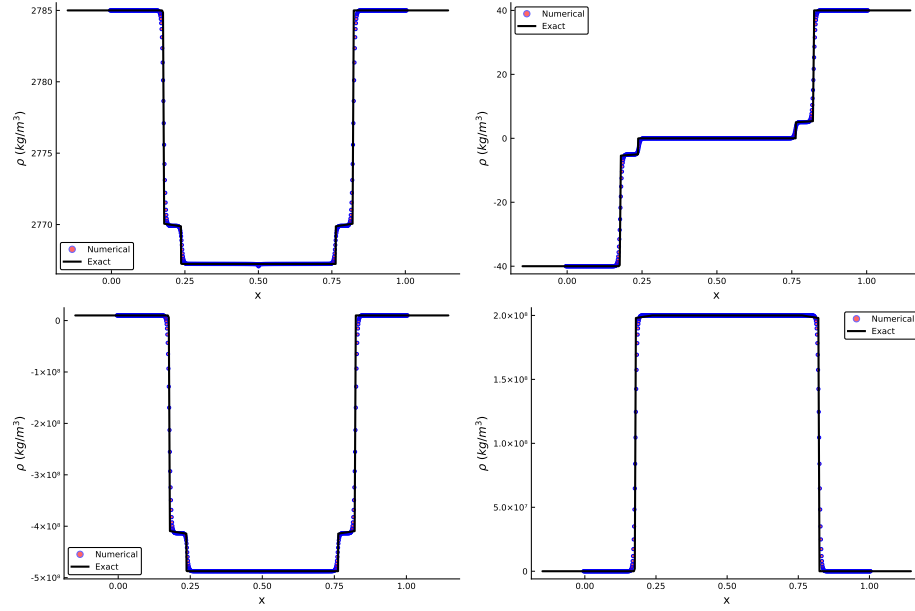Figure 8: Comparison resutls for Test 3 with the structrures of $R^E | R^E$.

Figure 9: Comparison resutls for Test 4 with the structrures of $R^E R^P | R^P R^E$.
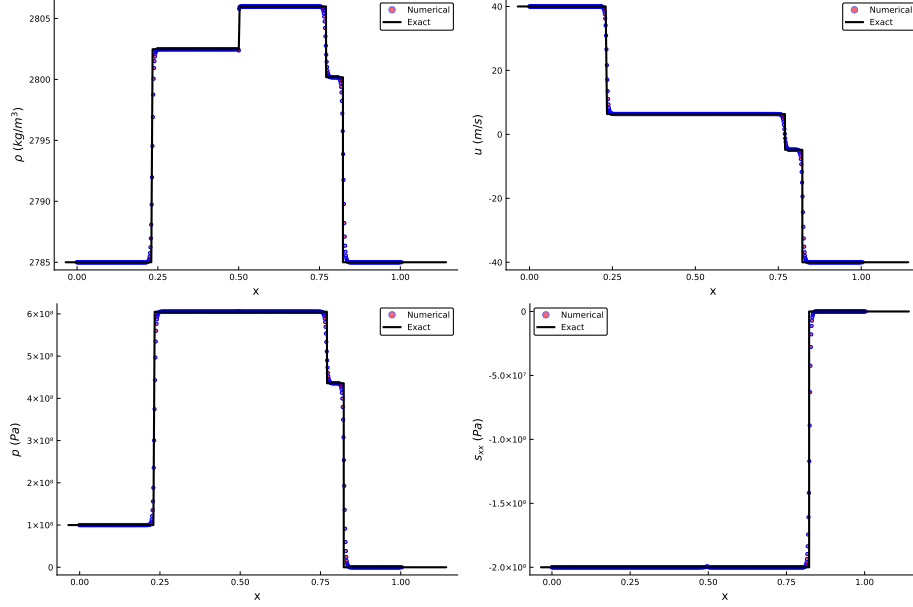
Figure 10: Comparison resutls for Test 5 with the structrures of $R^P|R^PR^E$.

6.5. Test 5

All the above four tests have symmetrical wave structrues, next we will test an example with different structrues on different sides. The initial condition is given as

$$
\begin{cases}
\text{L: Al,} & \rho = 2785\text{kg/m}^3, & u = 40\text{m/s,} & p = 1.0 \times 10^8\text{Pa,} & s_{xx} = -2.0 \times 10^8\text{Pa,} \\
\text{R: Al,} & \rho = 2785\text{kg/m}^3, & u = -40\text{m/s,} & p = 1.0 \times 10^2\text{Pa,} & s_{xx} = 0.0\text{Pa.}
\end{cases}
\tag{141}
$$

In the Fig.10 shown in both the numerical and exact solutions, there is one plastic shock on the left side and both the elastic and plastic shocks exist on the right.

6.6. Test 6

In this test, we consider an example with zero initial velocities on both sides, driving by the gradient of the pressure, there are rarefaction waves producted into the higher pressure side and shock waves generated into the lower pressure
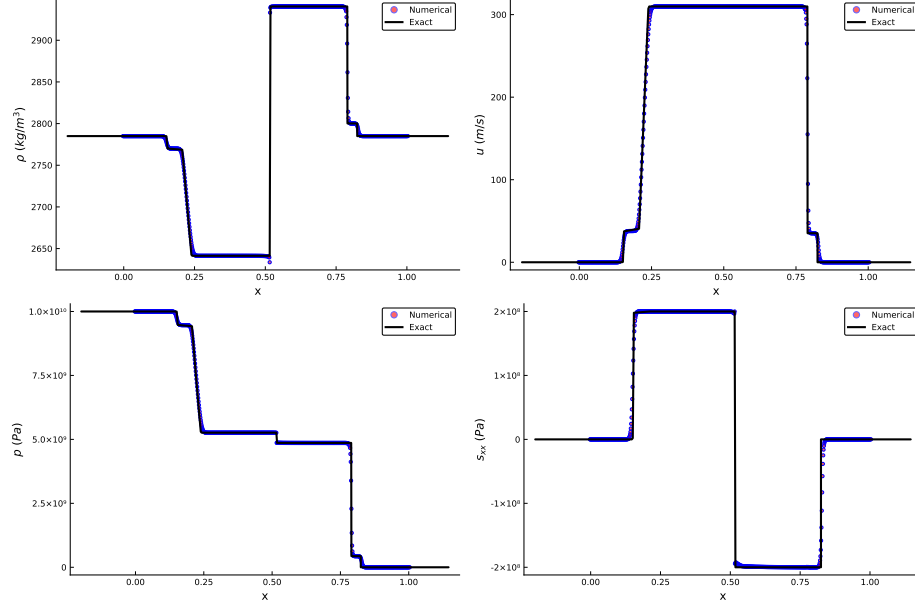
31

Figure 11: Comparison resutls for Test 6 with the structrures of $R^E R^P | S^P S^E$.

side. The initial condition is given as

$$
\begin{cases}
\text{L: Al,} & \rho = 2785\text{kg/m}^3, & u = 0.0\text{m/s}, & p = 1.0 \times 10^{10}\text{Pa}, & s_{xx} = 0.0\text{Pa}, \\
\text{R: Al,} & \rho = 2785\text{kg/m}^3, & u = 0.0\text{m/s}, & p = 1.0 \times 10^{2}\text{Pa}, & s_{xx} = 0.0\text{Pa}.
\end{cases}
$$
(142)

Shown in Fig.14, we can see there are two shocks in the right side and two rarefaction waves on the left side.

6.7. Test 7

Now we will consider two multi-material tests with different materials on different sides. In this test, on the left side, a lighter material of aluminum with a velocity impacts to a heavier material of copper. The initial condition is given as

$$
\begin{cases}
\text{L: Al,} & \rho = 2785\text{kg/m}^3, & u = 40\text{m/s}, & p = 0.1\text{Pa}, & s_{xx} = 0.0\text{Pa}, \\
\text{R: Copper,} & \rho = 8930\text{kg/m}^3, & u = 0.0\text{m/s}, & p = 0.1\text{Pa}, & s_{xx} = 0.0\text{Pa}.
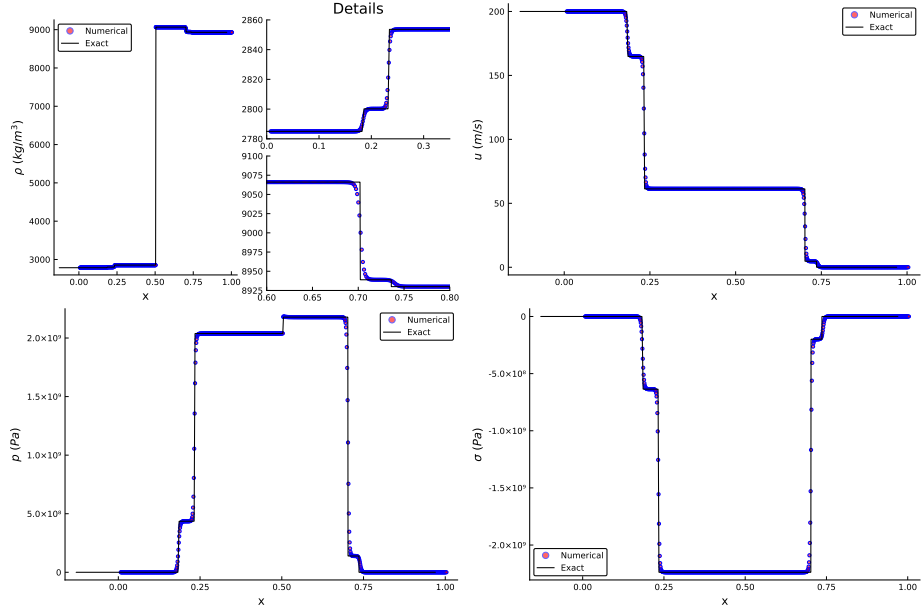\end{cases}
$$
(143)

32

Figure 12: Comparison results for Test 7 with structrures of $R^E R^P | R^P R^E$.

Show in the Fig.12, there is a large jump of density at the material interface and both elastic shock and plastic shock exist in each side of the interface. The exact Riemann solver can solve the Riemann problem with multi-materials very well comparing to the MHLLCEP approximate solver.

6.8. Test 8

At last, we test another multi-materials case, in this test the initial condtion is given as

$$
\begin{cases}
\text{L: Copper,} \quad \rho = 8930\text{kg/m}^3, \quad u = 0.0\text{m/s}, \quad p = 1.0 \times 10^{10}\text{Pa}, \quad s_{xx} = 0.0\text{Pa}, \\
\text{R: Al,} \quad \rho = 2785\text{kg/m}^3, \quad u = 0\text{m/s}, \quad p = 10.0\text{Pa}, \quad s_{xx} = 0.0\text{Pa}.
\end{cases}
\tag{144}
$$

Shown in Fig.13, there are two rarefaction waves on the left side and two shocks on the right side, there is a discontinuity of pressure on the interface, and the Cauchy stress is continuous, which meets with the theoretical analysis.
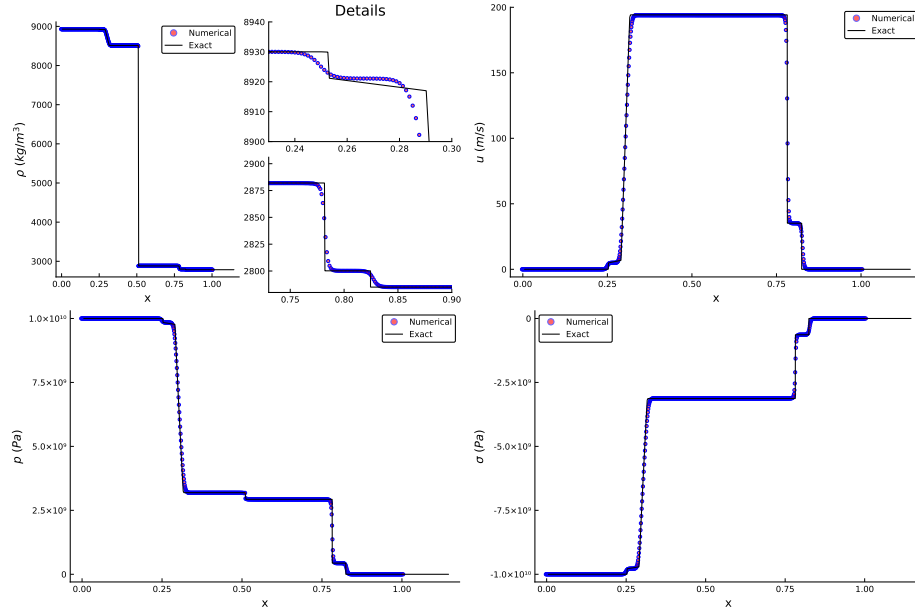
33

Figure 13: Comparison results for Test 8 with the structrures of $R^E R^P | S^E S^P$.

6.9. Test 9

Then we give two tests of half Riemann problem, the first is with a given left velocity $u^* = -20$m/s, and the right initial condition is

$$\text{Copper,} \quad \rho = 8930\text{kg/m}^3, \quad u = 0.0\text{m/s}, \quad p = 0.1\text{Pa}, \quad s_{xx} = 0.0\text{Pa}. \quad (145)$$

In Fig.14, comparason results are given by the exact half Riemann solver and the numerical method. We can see that the exact solver can resolve both the elastic and plastic shock waves well.

6.10. Test 10

The second half Riemann case is with a given left Cauchy stress $\sigma^* = 0$Pa, and the right initial condition is

$$\text{Copper,} \quad \rho = 8930\text{kg/m}^3, \quad u = 0.0\text{m/s}, \quad p = 1.0 \times 10^9\text{Pa}, \quad s_{xx} = 0.0\text{Pa}. \tag{146}$$
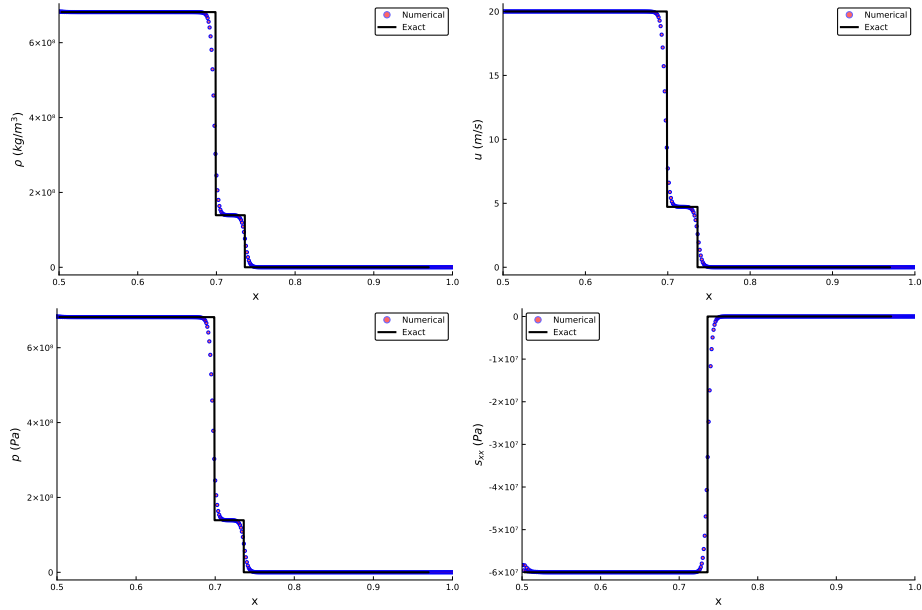
34

Figure 14: Comparison results for Test 9 with the structrures of $S^E S^P$.

In Fig.15, we give the results computed by the exact Riemann solver and the numerical simulation, shown in it, the exact solver can resolve the elastic and plastic rarefaction waves well.

References

[1] M. L. Wilkins, Calculation of elastic-plastic flow, Tech. rep., California Univ Livermore Radiation Lab (1963).

[2] S. L. Gavrilyuk, N. Favrie, R. Saurel, Modelling wave dynamics of compressible elastic materials, Journal of computational physics 227 (5) (2008) 2941–2969.
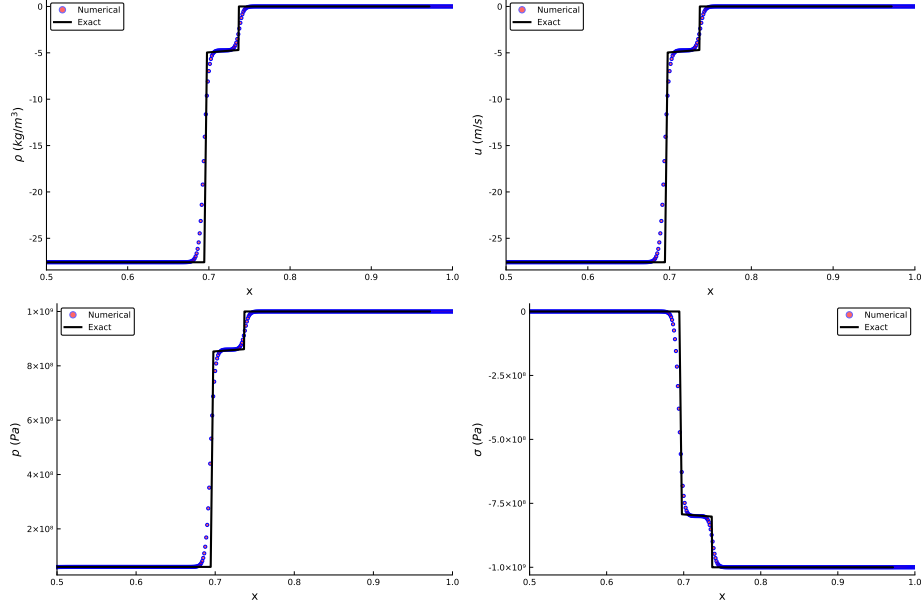
Figure 15: Comparison results for Test 10 with the structrures of $R^E R^P$.

[3] J.-B. Cheng, E. F. Toro, S. Jiang, M. Yu, W. Tang, A high-order cell-centered Lagrangian scheme for one-dimensional elastic–plastic problems, Computers & Fluids 122 (2015) 136–152.

[4] J. Cheng, Harten-Lax-van Leer-contact (HLLC) approximation Riemann solver with elastic waves for one-dimensional elastic-plastic problems, Applied Mathematics and Mechanics 37 (11) (2016) 1517–1538.

[5] L. Liu, J.-b. Cheng, A multi-material hllc riemann solver with both elastic and plastic waves for 1d elastic-plastic flows.

[6] S. K. Godunov, A difference method for numerical calculation of discontinuous solutions of the equations of hydrodynamics, Matematicheskii Sbornik 89 (3) (1959) 271–306.

[7] X. Garaizar, Solution of a Riemann problem for elasticity, Journal of elasticity 26 (1) (1991) 43–63.

[8] G. H. Miller, An iterative riemann solver for systems of hyperbolic conservation laws, with application to hyperelastic solid mechanics, Journal of Computational Physics 193 (1) (2004) 198–225.

[9] S. Gao, T. Liu, 1d exact elastic-perfectly plastic solid Riemann solver and its multi-material application, Advances in Applied Mathematics and Mechanics 9 (3) (2017) 621–650.

[10] S. Gao, T. Liu, C. Yao, A complete list of exact solutions for one-dimensional elastic-perfectly plastic solid riemann problem without vacuum, Communications in Nonlinear Science and Numerical Simulation 63 (2018) 205–227.

[11] L. Xiao, Numerical computation of stress waves in solids, Akademie Verlag Gmbh, Berlin.

[12] P.-H. Maire, R. Abgrall, J. Breil, R. LoubèRe, B. Rebourcet, A nominally second-order cell-centered Lagrangian scheme for simulating elastic–plastic flows on two-dimensional unstructured grids, Journal of Computational Physics 235 (2013) 626–665.